ELSEVIER

Physica C 382 (2002) 342–348

PHYSICA C

www.elsevier.com/locate/physc

Uniform texture in meter-long $YBa_2Cu_3O_7$ tape

E.D. Specht [a,*], F.A. List [a], D.F. Lee [a], K.L. More [a], A. Goyal [a], W.B. Robbins [b], D. O'Neill [b]

[a] *Oak Ridge National Laboratory, P.O. Box 2008, MS 6118, Oak Ridge, TN 37831-6118, USA*
[b] *3M Company, St. Paul, Minnesota 55144-1000, USA*

Received 6 November 2001; received in revised form 15 January 2002; accepted 18 January 2002

Abstract

A reel-to-reel tape handler mounted on a four-circle diffractometer is used to provide a characterization by X-ray diffraction of the entire 1 m length of a $YBa_2Cu_3O_7/CeO_2/Y_xZr_{1-x}O_2/CeO_2/Pd/Ni$ ($YBCO/CeO_2/YSZ/CeO_2/Pd/Ni$) tape. Cube-textured Ni was formed by rolling and annealing; epitaxial $CeO_2/YSZ/CeO_2/Pd$ buffer layers were deposited by reactive sputtering; YBCO was converted ex situ from Y, BaF_2, and Cu codeposited by e-beam evaporation. Rocking curve FWHM (mean ± standard deviation) for 95 segments of 1 cm length are: $YBCO(005) = 6.2 \pm 0.5°$, $YSZ(002) = 10.4 \pm 0.4°$, and $Ni(002) = 7.6 \pm 0.3°$. ϕ scan FWHM are: $YBCO(113) = 9.6 \pm 0.4°$, $YSZ(111) = 13.0 \pm 0.4°$, and $Ni(111) = 10.6 \pm 0.4°$. Greater than 95% of the tape at each point is cube textured from Ni to YBCO. The critical current density J_c is 0.36 ± 0.04 MA/cm^2 at 77 K and is inversely correlated with the rocking curve FWHM. Calculations suggest that J_c might be increased by a factor of 2.1 by producing a sharper texture and that the uniformity of the texture will support scaling to kilometer lengths.

PACS: 85.25.Kx; 74.72.Bk; 07.85.Jy
Keywords: Coated conductor; Texture; YBCO; Long length; RABiTS

1. Introduction

YBCO, which has high J_c at 77 K even in high-magnetic fields, is a promising superconductor for use in applications such as motors, transformers, and power transmission. Its performance is considerably degraded by high-angle grain boundaries [1], presenting a technical challenge in the production of long superconductors. Superconducting films with no high-angle grain boundaries are readily grown epitaxially on single-crystal substrates, but long YBCO conductors have been produced only by epitaxial growth on biaxially textured polycrystalline substrates or buffer layers [2,3], with both low- and high-angle grain boundaries [4]. Short tapes have been prepared with $J_c > 2 \times 10^6$ A/cm^2 [5,6], and meter-long tapes with $J_c = 1 \times 10^6$ A/cm^2 [2]. These J_c's are high, but many applications require kilometer lengths: how will J_c scale with tape length?

While there are no observations concerning YBCO conductors for kilometer lengths, the critical current for km-long conductors has been

* Corresponding author. Tel.: +1-865-574-7682; fax: +1-865-574-7659.
E-mail address: spechted@ornl.gov (E.D. Specht).

0921-4534/02/$ - see front matter
PII: S0921-4534(02)01248-0

calculated using a simplified model where a randomly located low-angle fraction of the grain boundaries all have the same J_c and the remaining high-angle boundaries are nonconducting; the supercurrent must percolate through the conducting boundaries [7,8]. These models show that if the fraction of conducting boundaries is high enough to give a high J_c for centimeter lengths, J_c will be only $\sim$10% lower for kilometer lengths. That is, there is a significant probability that a random bunching of high-angle boundaries will block most of the current only in cases where either the fraction of conducting grain boundaries or the width of the tape (relative to the grain size) is so low that even short samples are poorly conducting. There is no fundamental obstacle to long, crystallographically aligned tapes.

Can processing conditions be kept sufficiently uniform that the distribution of grain boundary angles is constant over the length of a tape? As a step toward answering this question, we present the first complete characterization of the texture of a meter-long superconducting tape. A reel-to-reel tape handler mounted on a four-circle diffractometer was used to obtain rocking curves and ϕ scans covering the entire length of the tape and $\theta/2\theta$ scans and pole figures at selected positions. These results are correlated with J_c measurements for each 1 cm segment of the tape.

2. Experimental

2.1. Sample preparation

Samples used in the ex situ conversion are prepared by co-evaporating Y, Cu and BaF_2 onto CeO_2/YSZ/CeO_2/Pd/Ni rolling-assisted, biaxially textured substrates (RABiTS^{TM}). Details of the RABiTS^{TM} fabrication processing are given elsewhere [9]. Briefly, long-length RABiTS^{TM} is prepared in a continuous, single pass, reel-to-reel process where a rolled Ni tape, 0.05 mm thick and 13 mm wide is recrystallized into a cube texture by annealing at 1050° C. Pd (1.5 nm), CeO_2 (24 nm), YSZ (160 nm) and CeO_2 (14 nm) buffer layers are deposited by reactive DC magnetron sputtering using metallic targets and Ar and H_2O as the sputtering and reactant gases, respectively. In this single pass arrangement, the entire RABiTS^{TM} substrate, including metal annealing and buffer depositions, is processed concurrently at a speed of 18 m/h. Following RABiTS^{TM} fabrication, the substrate is loaded into a three-gun reel-to-reel electron-beam evaporation system for precursor deposition. Source materials in the form of metallic Y and Cu and crystals of BaF_2 are used to deposit a film 350 nm in thickness and with Y/Ba/Cu composition of 0.93/2.09/3.00 as determined by inductively coupled plasma (ICP) analysis [10].

The meter-long precursor-coated RABiTS^{TM} is loaded into a reel-to-reel extended zone atmospheric furnace for conversion to YBCO. Details of the furnace and the conversion process can be found elsewhere [11]. Briefly, seven transverse-flow modules, each 30 cm long, are stacked end-to-end and incorporated into an Inconel 601 conversion chamber which is $2500 \times 5 \times 1$ cm^3 ($l \times w \times h$). Two Inconel 601 tubes serve as gas inlet and outlet ports within each flow module, each 1 cm in diameter with 125 μm holes. These tubes are welded in place in a transverse-flow geometry, with the sample between opposing input and output holes. The chamber is heated within a 22-zone furnace, with the sample spooled between reels at either end. Total pressures at the gas inlet, gas outlet and within the chamber, as well as oxygen activity are continuously monitored. The five upstream modules can be set to provide either a wet or dry gas environment, whereas the two downstream modules remain dry at all times. Ni leaders are spot welded to the meter-long sample, the furnace is preheated, and conversion to YBCO is conducted at a speed of 0.6 m/h in a single pass, with a wet conversion time of 120 min, a dry annealing time of 60 min, a conversion temperature of 740 °C, an O_2 partial pressure of 130 mTorr, an H_2O partial pressure of 70 Torr, and a gas flow rate of 5.5 l/min.

Following conversion to YBCO, a 1 μm thick silver cap layer is deposited onto the YBCO film by reel-to-reel DC magnetron sputtering. The sample is then annealed at 500 °C in flowing O_2 to oxygenate the YBCO and to decrease the contact resistance between Ag and YBCO. Sectional J_c measurement at 1 cm increments is performed at

77 K and self-field using standard four-probe configuration and a 1 μV/cm criterion.

Cross-sectional transmission electron microscopy with energy-dispersive X-ray analysis was used to locate and identify phases in a similarly prepared short sample.

2.2. Texture measurement

The sample was mounted for X-ray diffraction on a reel-to-reel handler bolted to the ϕ stage of a Huber four-circle diffractometer as shown in Fig. 1. Up to 20 m of 12.5×0.05 mm^2 tape can be spooled on reels 10 cm in diameter. The inside diameter of the χ circle is 40 cm, providing clearance for 360° rotation of χ and ϕ. One reel is controlled by a microstepping motor, the other is driven by a constant-torque motor. The sample slides across stainless steel guides with a 10 cm radius which keep the tape at a constant height between the guides, where it is irradiated.

A Cu rotating anode source operates at 5 kW. A bent, sagitally focusing graphite (0 0 2) monochromator selects K_α fluorescence, and collimation is provided by a 75 cm flight path upstream of a 2.5 mm wide × 5 mm high-entrance slit. Diffracted radiation is collimated by soller slits. These parallel-beam optics make the measurements insensitive to small changes in the sample position. This system was an adaptation of one built for other uses; we are currently building a dedicated system in which higher intensity is obtained by placing the X-ray source much closer to the sample and using a parabolically bent variable-period multilayer to both collimate and monochromate the incident beam.

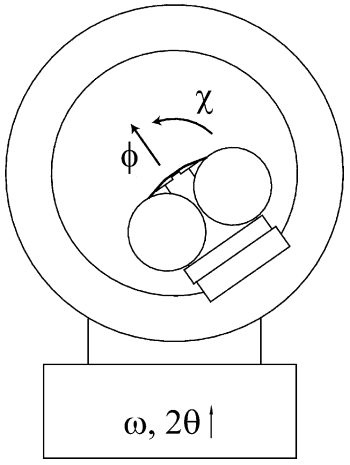

Fig. 1. Reel-to-reel tape handler mounted on four-circle diffractometer. Reel diameter is 10 cm, χ circle ID is 40 cm.

At an incident angle of $2\theta/2 = 15°$, the footprint of the 2.5-mm-wide beam is 2.5 mm/sin 15° = 1 cm. Thus texture measurements were repeated at 1 cm intervals to cover the entire tape with one for each J_c segment. Out-of-plane texture was measured by rocking curves (ω scans) taken by rotating the sample about both the rolling direction (ω_R) and the cross direction (ω_C). The FWHM $\Delta\omega$ and $\Delta\phi$ are calculated from least-squares fitting to a Gaussian lineshape. In-plane texture was inferred from ϕ and ω scans [12]. For Ni(1 1 1) and YSZ(1 1 1) ϕ scans, the four reflections at an azimuth 45° to the rolling direction are symmetry equivalent and the in-plane width is

$$\Delta\Phi = \sqrt{\Delta\phi^2 - \tan^2\chi(\Delta\omega_R^2 + \Delta\omega_C^2)/2}, \quad (1)$$

where $\chi = 35°$ is the inclination of the reflections. For YBCO(1 1 3), the reflections at the azimuth of the rolling and cross directions are not equivalent; we measure at the azimuth of the cross direction and compute

$$\Delta\Phi = \sqrt{\Delta\phi^2 - \tan^2\chi\Delta\omega_C^2}. \quad (2)$$

Data were collected for the Ni substrate, the YSZ buffer layer, and the YBCO superconductor. The CeO_2 cap is consumed during the formation of YBCO; scattering from the buried CeO_2 and Pd layers is too weak to collect useful data.

To see whether textures other than the (0 0 1)[1 0 0] cube texture are present, we perform "tape scans", in which we hold the sample and detector orientation fixed at the Bragg reflection angles for cube texture and count scattered X-rays while scanning the tape position. Where other textures are present, the cube texture intensity will decrease. Other factors which may affect the intensity are the sharpness of the cube texture, the thickness of the superconducting layer, and the presence of other phases or amorphous material. Having identified possible locations of unwanted

texture, we determine the magnitude of the cube texture fraction from pole figures collected at these positions on the tape. YBCO(113), YSZ(1 1 1), and Ni(1 1 1) pole figures are collected using the Schultz reflection geometry [13]. Volume fraction is computed by integrating pole intensity using an equal-area projection; the integrated intensity of the cube texture peaks is compared to the total integrated intensity. We define "cube texture" to be orientations where $(\Delta\phi/30°)^2 + (\Delta\omega/25°)^2 < 1$; $\Delta\phi$ and $\Delta\omega$ are the in-plane and out-of-plane angular deviations from the nearest cube texture orientation. $\theta/2\theta$ scans were collected at selected points on the tape to analyze chemical phase. Tape scans were made at the Bragg angle of each secondary phase.

3. Results and discussion

The J_c for each 1 cm section of the tape is shown in Fig. 2. The sectional J_c is 0.36 ± 0.04 MA (mean $\pm$ standard deviation). There are small deficits near 20 and 83 cm. In the rest of this paper we will focus on possible causes of this variation. The mosaic spread varies little over the length of the tape (Table 1 and Fig. 3); the decrease in J_c near 83 cm is associated with a broadening of the mosaic for all layers, while the decrease near 20 cm is not.

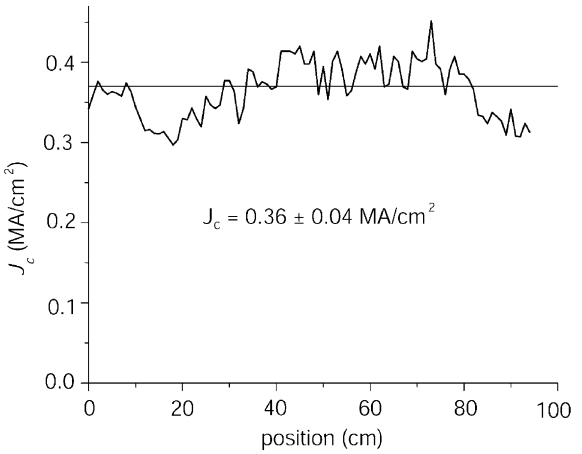

Fig. 2. J_c, measured for each 1 cm segment.

Table 1
Mean, standard deviation, and maximum FWHM (deg)

Layer		Ni	YSZ	YBCO
Rocking curve $\Delta\omega_C$	Mean	7.62	10.35	6.24
	SD	0.30	0.37	0.47
	Max	9.79	12.30	8.85
Rocking curve $\Delta\omega_R$	Mean	11.10	15.36	8.07
	SD	0.31	0.95	0.52
	Max	11.89	17.89	9.86
ϕ scan $\Delta\phi$	Mean	10.58	12.97	9.62
	SD	0.40	0.38	0.36
	Max	12.81	13.95	11.01
In-plane mosaic $\Delta\Phi$ (Eq. (2))	Mean	8.21	9.13	8.56
	SD	0.51	0.63	0.32
	Max	10.47	11.19	9.95

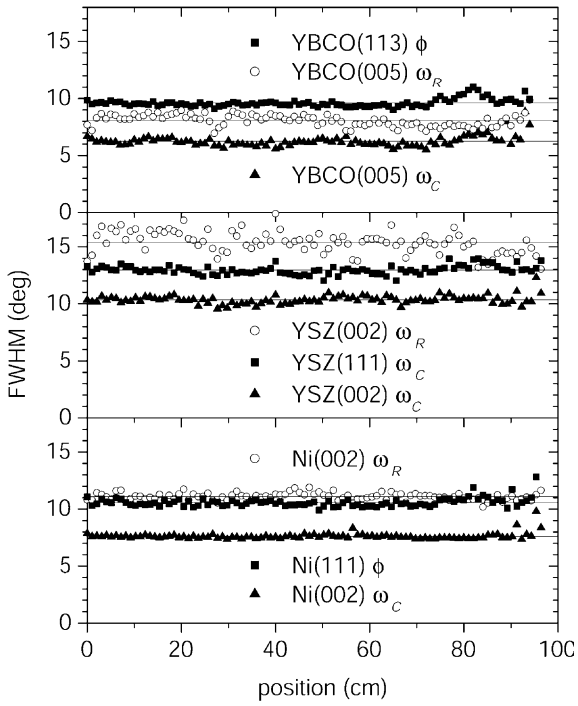

Fig. 3. ϕ scan and rocking curve widths.

A $\theta/2\theta$ scan at the tape midpoint (Fig. 4) shows cube-textured Ni, CeO_2, YSZ, and YBCO, along with NiO, $Y_2Cu_2O_5$, and $BaCeO_3$. TEM shows that NiO grows at the interface between Pd/Ni and CeO_2 when the O_2 pressure is raised for YBCO

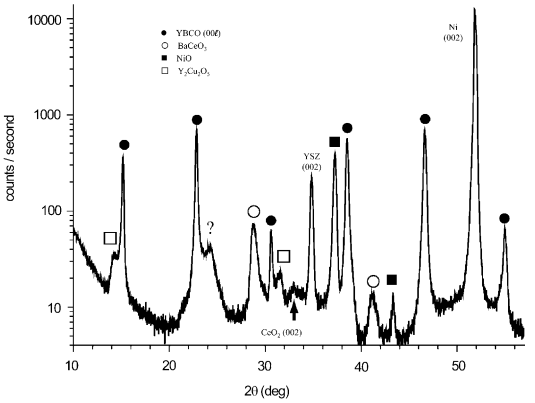

Fig. 4. $\theta/2\theta$ scan at tape midpoint. $BaCeO_3$ peaks are also consistent with BaF_2, and the peak marked '?' may also be due to BaF_2.

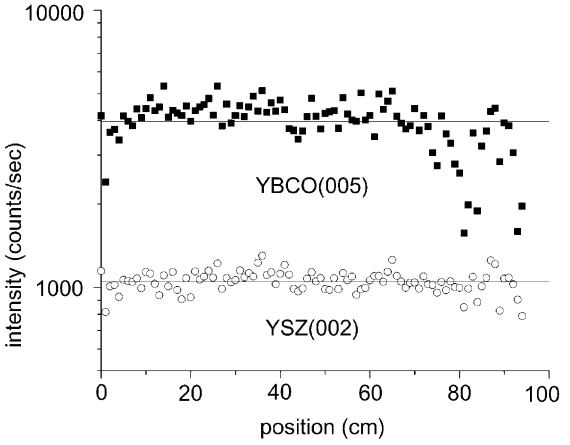

Fig. 5. Intensity from cube-texture Bragg reflections.

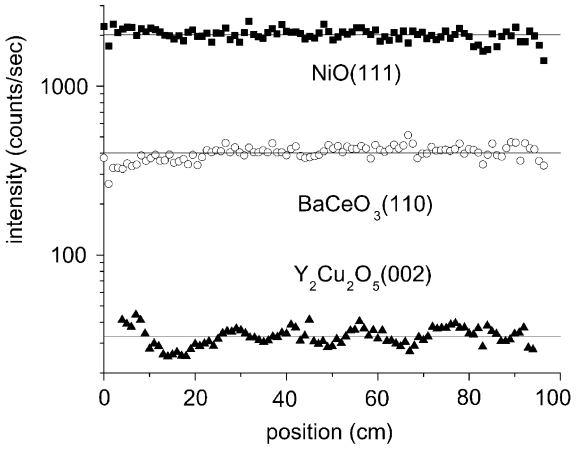

Fig. 6. Bragg intensity from reaction products.

formation. The uppermost CeO_2 layer is entirely consumed, leaving a continuous $BaCeO_3$ layer 30 nm thick; reaction of CeO_2 with BaF_2 accounts for the observed $BaCeO_3$ as a reaction product. Ellipsoidal $Y_2Cu_2O_5$ particles ranging in size from 50 to 100 nm are found throughout the YBCO film. Reaction of CeO_2 with BaF_2 would leave excess Y and Cu, which will react under oxidizing conditions to form $Y_2Cu_2O_5$. The $BaCeO_3$ X-ray reflections exhibit broadening which corresponds to a 12 nm grain size, while the other reflections are at instrumental resolution, indicating >30 nm particle size.

The YSZ(0 0 2) Bragg intensity varies by only 9% over the length of the tape, but YBCO has large decreases in intensity near 83 and 94 cm (Fig. 5). The decrease at 83 cm is associated with a broadening of the YBCO mosaic (Fig. 3), but this does not occur at 94 cm, indicating that there is a deficit of cube-textured YBCO at this point. The intensity of NiO diffraction shows the diffusion of oxygen to the Ni substrate occurs uniformly over the length of the tape (Fig. 6). Fig. 7 compares pole figures at points of higher (40 cm) and lower (20 and 83 cm) J_c. While the YBCO Bragg intensity is lower at 83 cm (Fig. 6), the fraction of cube texture remains unchanged (Table 2); only the mosaic of the cube texture changes. Retained rolling texture is observed in Ni, while YSZ and YBCO have grains rotated 45° from the majority phase. The variations in the fraction of cube texture does not vary significantly, either between layers or between segments, which suggests that the 45° rotated grains form on regions with retained rolling texture.

Multivariate regression analysis was done to determine the effect of all the texture variables on J_c and all possible interaction terms such as the effect of out-of-plane texture on in-plane texture, etc. Nine texture variables were considered in all. The best fits for all possible combinations of variables was identified. Statistical tests such as the student t-test, the p-value of the predicted coeffi-

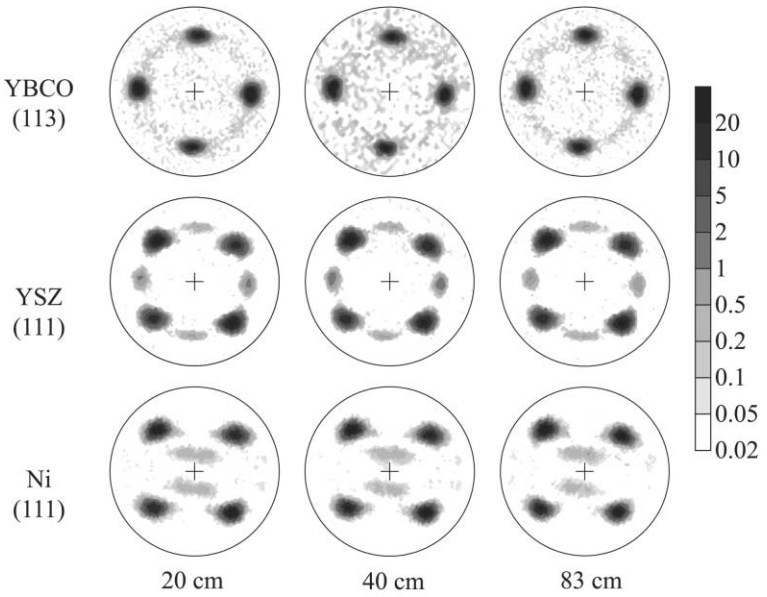

Fig. 7. Log-scale, background-subtracted pole figures.

Table 2
Fraction without cube texture

	20 cm	40 cm	83 cm
YBCO(1 1 3)	2.8%	2.7%	2.9%
YSZ(1 1 1)	3.9%	3.4%	4.7%
Ni(1 1 1)	2.8%	2.6%	2.5%

cients and the *f*-test for the regression analysis were performed to determine the statistically significant coefficients. It was determined that the texture variables account for only 20% of the variation in the J_c as a function of length. Extending the analysis to include secondary phases increased the number of possible variables to 12. It was determined that inclusion of the secondary phases in the analysis, could still only explain ~38% of the variation in the J_c-data as a function of length.

Texture accounts for only some of the low-frequency variation in J_c: the decrease near 83 cm but not that near 20 cm. We have demonstrated that epitaxial YBCO films can be grown on textured polycrystalline substrates with great uniformity. The degree of cube texture is uniform and high. The sharpness of that texture exhibits only minor variations, decreasing J_c by only ~15%.

The texture of this tape is far from optimum: the Ni substrate has a mean in-plane mosaic $\Delta\Phi = 8.21°$ FWHM (Table 1). The epitaxy is effective: the YBCO texture is actually sharper than that of Ni. Cube-textured Ni has been prepared in short lengths with $\Delta\Phi$ low as 5.0° FWHM [12]; efforts are underway to produce this texture reproducibly in long lengths. As the texture sharpens from 8.21° to 5.0°, the fraction of grain boundaries with <5° misorientation increases from 69% to 90%, and we would expect J_c to increase by a factor of 2.1; i.e. from 0.37 to 0.78 MA/cm^2 [7]. Formation of cube-textured YBCO is not entirely uniform; optimization of the reaction conditions, improved tape handling, and better process control will be required for maximum J_c over long lengths. But if we extrapolate the 0.38 ± 0.05 MA/cm^2 variation in J_c measured for this tape to a length of 1 km, assuming Gaussian statistics, each segment will still have $J_c > 0.23$ MA/cm^2. CeO_2/YSZ/CeO_2/Pd/Ni substrates have been prepared without significant variation in mosaic spread over a 1 m length, and appear ready for scale-up.

4. Conclusion

A method for exhaustively characterizing the texture of coated conductor tape in lengths up to 20 m has been applied to a meter-long YBCO film grown on roll-textured Ni buffered with YSZ and CeO_2. The mosaic of substrate and epitaxial films varies by only $\sim 0.5^\circ$ over the length of the tape; this variation in texture accounts for only $\sim 20\%$ of the variation in J_c. Statistical extrapolation of the texture fluctuations suggests that the texture will support high J_c over kilometer lengths.

Acknowledgements

Work sponsored by the Department of Energy, Division of Materials Sciences and Office of Energy Efficiency and Renewable Energy, Office of Power Technologies, Superconductivity Program. Oak Ridge National Laboratory (ORNL) is operated by UT-Battelle, LLC, for the US Department of Energy under contract DE-AC05-00OR22725. We have benefited from helpful discussions with Noel Rutter.

References

[1] D. Dimos, P. Chaudhari, J. Mannhart, F.K. LeGoues, Phys. Rev. Lett. 61 (1988) 219.
[2] S.R. Foltyn, P.N. Arendt, P.C. Dowden, R.F. DePaula, J.R. Groves, J.Y. Coulter, Q. Jia, M.P. Maley, D.E. Peterson, IEEE Trans. Appl. Supercond. 9 (1999) 1519.
[3] M. Paranthaman, T.G. Chirayil, S. Sathyamurthy, D.B. Beach, A. Goyal, F.A. List, D.F. Lee, X. Cui, S.W. Lu, B. Kang, E.D. Specht, P.M. Martin, D.M. Kroeger, R. Feenstra, C. Cantoni, D.K. Christen, IEEE Trans. Appl. Supercond. 11 (2001) 3146.
[4] A. Goyal, S.X. Ren, E.D. Specht, D.M. Kroeger, R. Feenstra, D.P. Norton, M. Paranthaman, D.F. Lee, D.K. Christen, Micron 30 (1999) 463.
[5] D.T. Verebelyi, D.K. Christen, R. Feenstra, C. Cantoni, A. Goyal, D.F. Lee, M. Paranthaman, P.N. Arendt, R.F. DePaula, J.R. Groves, C. Prouteau, Appl. Phys. Lett. 76 (2000) 1755.
[6] J.E. Mathis, A. Goyal, D.F. Lee, F.A. List, M. Paranthaman, D.K. Christen, E.D. Specht, D.M. Kroeger, P.M. Martin, Jpn. J. Appl. Phys. 37 (1998) L1379.
[7] E.D. Specht, A. Goyal, D.M. Kroeger, Supercond. Sci. Technol. 13 (2000) 592.
[8] N.A. Rutter, B.A. Glowacki, J.E. Evetts, Supercond. Sci. Technol. 13 (2000) L25.
[9] W.B. Robbins, in: International Workshop on Superconductivity, ISTEC/MRS, Honolulu, Hawaii, 2001.
[10] M. Paranthaman, C. Park, X. Cui, A. Goyal, D.F. Lee, P.M. Martin, T.G. Chirayil, D.T. Verebelyi, D.P. Norton, D.K. Christen, D.M. Kroeger, J. Mater. Res. 15 (2000) 2647.
[11] D.F. Lee, in: International Workshop on Superconductivity, ISTEC/MRS, Honolulu, Hawaii, 2001.
[12] E.D. Specht, A. Goyal, D.F. Lee, F.A. List, D.M. Kroeger, M. Paranthaman, R.K. Williams, D.K. Christen, Supercond. Sci. Technol. 11 (1998) 945.
[13] L.G. Schultz, J. Appl. Phys. 20 (1949) 1030.